INT. J. NUM. METH. HEAT FLUID FLOW, VOL. 5, 781–795 (1995)

THERMAL AND FLUID-DYNAMIC BEHAVIOUR OF DOUBLE-PIPE CONDENSERS AND EVAPORATORS – A NUMERICAL STUDY

F. ESCANES, C. D. PÉREZ-SEGARRA AND A. OLIVA

Laboratori de Termotècnia i Energètica, Dept. Màquines i Motors Tèrmics, Universitat Politècnica de Catalunya, Colom 9, E-08222 Terrassa (Barcelona), Spain

ABSTRACT

This paper deals with a numerical simulation of the thermal and fluid-dynamic behaviour of double-pipe condensers and evaporators. The governing equations of the fluid flow (continuity, momentum and energy) in both the tube (evaporating or condensing flow) and the annulus (single-phase flow), together with the energy equation in the tube wall, are solved iteratively in a segregated manner using a one-dimensional, transient formulation, based on an implicit step by step numerical scheme in the zones with fluid flow (tube and annulus), and an implicit central difference numerical scheme in the tube wall, solved by means of the Tri-Diagonal Matrix Algorithm (TDMA). This formulation requires the use of empirical information for the evaluation of convective heat transfer, shear stress and void fraction. Two criteria to calculate the location of the points of transition between single-phase and two-phase flow are tested. An analysis of the different parameters used in the discretization is made. Some illustrative results corresponding to the solution of a condenser and an evaporator using two different working fluids (R-12 and R-134a) are presented.

KEY WORDS Heat exchanger Condenser Evaporator Numerical simulation

NOMENCLATURE

c_p	specific heat at constant pressure
D	diameter
f	friction factor
g	gravity acceleration
h	specific enthalpy
e	specific energy defined as: $e=h+v^2/2+gz\cdot\sin\theta$
L	length
m	mass
$\dot{m}$	mass flow rate
n	number of control volumes
p	pressure
P	perimeter
$\dot{q}$	heat flux
r	radial coordinate
S	cross-section
t	time
T	temperature
v	velocity
x_g	vapour quality
z	axial coordinate

Greek symbols

α	convective heat transfer coefficient
δ	rate of convergency
Δh_{fg}	latent heat
Δt	time discretization step
Δz	spatial discretization step
λ	thermal conductivity
ε_g	void fraction
ϕ	generic dependent variable
θ	inclination angle
ρ	density
τ	shear stress
ζ	roughness

0961–5539/95/090781–16$2.00

Received February 1994
Revised September 1994

Subscript

b	boundary
bc	beginning of condensation
ec	ending of condensation
g	gas, vapour
i	inlet; inlet cross-section of a fluid control volume; index grid node
l	liquid
o	outlet; outlet cross-section of a fluid control volume
sat	saturation
tp	two-phase
W, P, E	grid points in the tube (*Figure 4*)
n, s, e, w	faces of a tube wall control volume (*Figure 4*)

Superscript

o	preceding instant
–	arithmetic average over a control volume: $\bar{\phi}=(\phi_i+\phi_{i+1})/2$
~	integral average over a control volume: $\tilde{\phi}=(1/\Delta z)\int_z^{z+\Delta z}\phi\,dz$

INTRODUCTION

In order to optimize the efficiency of the heat exchangers, and consequently the energy consumption, accurate methods of prediction for their behaviour are required. All of which is particularly applicable to situations involving two-phase flow inside tubes as in the cases of double-pipe and shell and tube condensers and evaporators among others.

The inherent complexity of the heat exchanger design in aspects such as complex geometries and fluid flow patterns, means that the possibilities of analytical solutions are very limited without assuming stringent simplifications (e.g. analytical approaches such as F-factor, ε-NTU, etc.). On the other hand, the use of numerical methods allows the governing equations to be solved with fewer restrictions.

Change of phase liquid-vapour inside tubes

Both the evaporating and condensing flows inside tubes are generally characterized by three different phenomena: single-phase vapour flow, two-phase flow, and single phase liquid flow. These three phenomena define three main regions: vapour region, two-phase region and liquid region (cf. *Figure 1*). The three regions are:

Liquid region (I): in the condenser this region corresponds to subcooled liquid. In the evaporator it can be divided into two subregions: subcooled liquid, and subcooled boiling (where the liquid temperature is lower than the saturation temperature and vapour bubbles begin to form at the wall proximities[1]).

Two-phase region (II): in the condenser this region corresponds to saturated liquid + vapour. In the evaporator it can be divided into two subregions: saturated liquid + vapour, an post-dryout regime (at low liquid quality, from a certain point called point of dryout, the liquid phase detaches

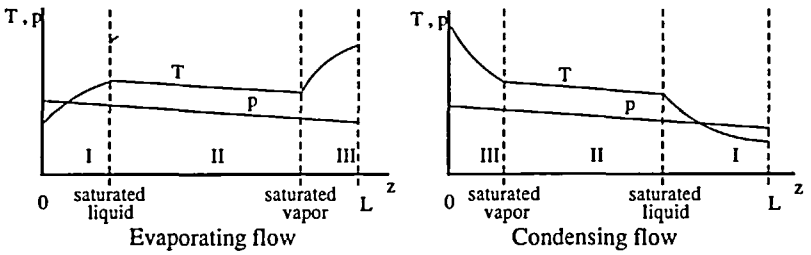

Figure 1 Typical temperature and pressure distribution for the change of phase liquid-vapour inside tubes. Characteristic regions: liquid region (I), two-phase region (II) and vapour region (III)

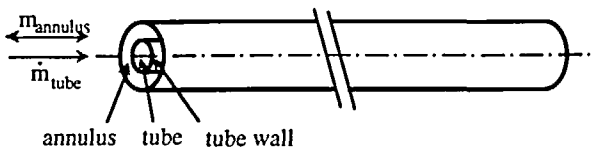

Figure 2 Double-pipe heat exchanger scheme

from the wall and travels inside the vapour core as liquid droplets; progressively the vapour temperature increases from the saturation temperature while the liquid droplets evaporate at the saturation temperature[1]).

Vapour region (III): in both the condenser and the evaporator this region corresponds to superheated vapour.

Both the subcooled boiling and the post-dryout regime in the evaporating flow strongly affect the flow pattern, so significant changes in the shear stress, the convective heat transfer and the flow structure are produced.

Objectives and methodology

The objective is to implement and develop numerical criteria which allow a simulation in both transient and steady state, of the thermal and fluid-dynamic behaviour of double-pipe condensers and evaporators, with two-phase flow inside the tube and single phase flow inside the annulus.

At each time step, the one-dimensional governing equations for each zone of the heat exchanger (flow inside the tube, flow inside the annulus, and tube wall, cf. *Figure 2*) are solved iteratively, in a segregated manner, using a fully implicit numerical scheme.

In the zones with fluid flow, the solution process is carried out, at each instant, moving forward step by step in the flow direction. In each control volume, beginning with the first one (duct inlet), given the flow variables at the inlet section, and at the preceding instant in the whole control volume, the solution of the set of discretized governing equations gives the flow variables at the outlet section. The flow variables at the inlet section of the control volume are boundary conditions for the first control volume, and the solution of the preceding control volume for the rest. The friction, the convective heat transfer and the void fraction are evaluated, at each cross section of the duct, by means of empirical correlations obtained from the available bibliography, taking into account the different flow regimes produced: single phase flow, evaporating and condensing flows, subcooled boiling and post-dryout subregion.

The energy equation governing the heat conduction in the tube wall is numerically solved over the discretized domain, using a central-difference numerical scheme[2]. The resulting set of discretized equations is solved through the algorithm TDMA[2]. The heat exchanged between the annulus flow and the surrounding ambient has been neglected, therefore it is not necessary to solve the energy equation in the external tube.

For the given boundary conditions, the modelization developed evaluates the distribution of the flow variables along the heat exchanger in both the tube and the annulus (temperature, pressure, velocity, etc.), and the temperature distribution in the tube wall. The characteristic parameters that define a specific situation to be analyzed are:

- *Geometry:* length, roughness, inside diameter of the tube, diameters of the annulus, flow arrangement (cocurrent flow or counter flow).
- *Boundary conditions:* temporal distribution of the inlet temperature or vapour quality, pressure and velocity in both the tube and the annulus; axial heat flux or temperature at the ends of the tube.
- *Initial conditions:* values of all dependent variables at each grid point at $t=0$.
- *Thermophysical properties* of the fluids and the tube wall material.

The next section describes the mathematical formulation of the governing equations over finite control volumes, in the particular case of the two-phase flow inside ducts and tubular wall elements. Next, different aspects of the numerical solution are shown in order to describe how the algorithm works. Finally, some illustrative results corresponding to the solution of a condenser and an evaporator working with two different fluids (R-12 and R-134a) are presented.

MATHEMATICAL FORMULATION

In this section the mathematical formulation of both the two-phase flow inside a characteristic control volume of a duct (single-phase flow, liquid or gas, represents a particular case), and the heat conduction in a tube wall element are presented.

The mathematical formulation of the fluid flow is made neglecting the difference of the liquid and vapour temperatures in the subcooled boiling and post-dryout regime in the evaporating flow. Their effects are considered through the use of empirical correlations for the evaluation of the shear stress, the convective heat transfer and the flow structure, adequate to the flow patterns produced.

Two-phase flow inside ducts

A characteristic control volume is shown schematically in *Figure 3*, where '*i*' and '*o*' represent the inlet and outlet sections respectively.

Taking into account the characteristic geometry of ducts in double-pipe heat exchangers, the governing equations have been integrated assuming the following hypotheses:

- One-dimensional flow: $T(z,t)$, $p(z,t)$, $v_g(z,t)$, $v_l(z,t)$, ...
- Fluid: pure substance; newtonian behaviour.
- Non-participant radiation medium and negligible radiant heat exchange between surfaces.
- Negligible axial heat conduction inside the fluid.
- Constant cross-section.

Integrating the governing equations over a finite control volume (see *Figure 3*) and neglecting second order terms, the following equations are obtained for two-phase flow:

- *Continuity:*

$$\dot{m}_i = \dot{m}_0 + \frac{\partial m}{\partial t} \tag{1}$$

- *Momentum:*

$$(p_i - p_0)S - \tilde{\tau} P \Delta z - m g \sin\theta = \dot{m}_{g,o} v_{g,o} - \dot{m}_{g,i} v_{g,i} + \dot{m}_{l,o} v_{l,o} - \dot{m}_{l,i} v_{l,i} + \Delta z \frac{\partial \tilde{m}}{\partial t} \tag{2}$$

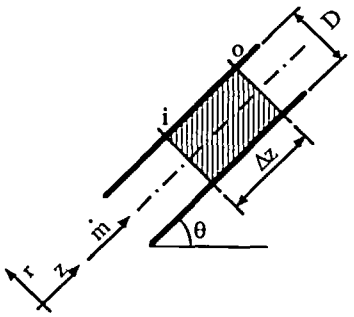

Figure 3 Flow inside a control volume

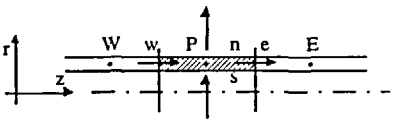

Figure 4 Heat fluxes in a control volume of the tube wall

where the evaluation of the shear stress is done by means of the two-phase friction factor f_{tp}, which is usually calculated using empirical correlations. This factor is defined from the expression: $\tau=(f_{tp}/4)(\dot{m}^2/2\rho_{tp}S^2)$.

- *Energy:*

$$\tilde{q}P\Delta z=\tilde{m}(e_{l,o}-e_{l,i})+\dot{m}_{g,o}(e_{g,o}-e_{l,o})-\dot{m}_{g,i}(e_{g,i}-e_{l,i})$$
$$+(\tilde{e}_g-\tilde{e}_l)\frac{\partial m_g}{\partial t}+m_g\frac{\partial \tilde{e}_g}{\partial t}+m_l\frac{\partial \tilde{e}_l}{\partial t}-S\Delta z\frac{\partial \tilde{p}}{\partial t}+(\tilde{e}_l-\bar{e}_e)\frac{\partial m}{\partial t} \quad (3)$$

where the specific energy is defined as $e=h+v^2/2+gz\sin\theta$. The last term in the energy equation is null for a differential control volume, and usually negligible for a finite control volume. In order to relate the convective heat transfer and the wall temperature, the convective two-phase heat transfer coefficient α_{tp} is introduced, which is defined from the equation: $\dot{q}=\alpha_{tp}(T_{wall}-T_{fluid})$.

This mathematical model requires information about the friction factor f_{tp}, and the convective heat transfer coefficient α_{tp}, together with the knowledge of the flow structure, that is, the volume occupied by the liquid and vapour phases. In order to evaluate it, the void fraction ε_g is a widely used parameter, defined as the time-averaged volume fraction of the vapour phase in the mixture (or the time-averaged area fraction of the vapour phase in a given cross-section), which can be expressed in terms of the gas to liquid velocity ratio v_g/v_l in the form[3]: $\varepsilon_g=(1+(1-x_g)\rho_g v_g/x_g\rho_l v_l)^{-1}$, where x_g is the vapour quality.

The balances mentioned above do not give information about the void fraction. This information is generally obtained from empirical information.

The flow of liquid or gas without change of phase can be analyzed as particular cases of this formulation.

Heat conduction in the tube wall

The conduction equation has been written assuming the following hypotheses:

- One-dimensional temperature distribution.
- Negligible heat exchanged by radiation.

A characteristic control volume is shown in *Figure 4*, where '*P*' is the central node, and '*E*' and '*W*' represent the neighbours, '*e*', '*w*', '*n*' and '*s*' are the faces of the control volume.

Integrating the energy equation over the control volume shown in *Figure 4*, the following equation is obtained:

$$(\tilde{q}_sP_s-\tilde{q}_nP_n)\Delta z+(\dot{q}_w-\dot{q}_e)S=m\frac{\partial \tilde{h}}{\partial t} \quad (4)$$

where $\tilde{q}_n$ and $\tilde{q}_s$ are evaluated using the respective convective heat transfer coefficients, and the conductive heat fluxes are evaluated from the Fourier law, that is: $\dot{q}_e=-\lambda_e(\partial T/\partial z)_e$ and $\dot{q}_w=-\lambda_w(\partial T/\partial z)_w$.

NUMERICAL SOLUTION

The numerical simulation developed allows the determining, in transient and steady state situations, of the distribution of pressures, temperatures, velocities, heat fluxes, etc. in double-pipe condensers and evaporators. It has been performed within a global algorithm that solves iteratively, in a segregated manner, the different zones: the evaporating or condensing flow inside the tube, the flow inside the annulus and the tube wall. The domain is divided into control volumes. For each control volume, a set of algebraic equations is obtained by a discretization of the governing equations (1) to (4).

In the fluid flow zones, the values of the flow variables at the outlet section of each control volume are obtained by solving the resulting set of algebraic equations, from the known values at the inlet section and at the preceding instant in the whole control volume. The solution procedure is carried out in this manner, moving forward step by step in the flow direction. At each cross section, the shear stresses, the convective heat fluxes and the void fraction are evaluated from empirical correlations obtained from the available literature. The solution scheme requires the knowledge of values of the flow variables at both the tube inlet and the annulus inlet as boundary conditions.

In the tube wall, the discretization of the energy equation gives a set of algebraic equations whose coefficients matrix is tri-diagonal. The resolution of this set of equations has been performed using the algorithm TDMA[2]. At the ends of the tube wall ($z=0$ and $z=L$) the temperature or the axial heat flux is specified as a boundary condition.

Spatial and temporal discretization procedure

Figure 5 shows the spatial discretization. The discretization nodes are located at the inlet and outlet sections of the control volumes in the fluid flow zones, while the discretization nodes are centered in the control volumes in the tube wall. Each zone contains n control volumes of length Δz.

The transitory solution is made every time step Δt. Depending on the time evolution of the boundary conditions, a constant or variable value of Δt can be selected.

Discretization equations

In the section *mathematical formulation*, the governing equations have been directly presented on the basis of the spatial integration over finite control volumes. Thus, only their temporal integration is required. A fully implicit scheme has been used. The transient terms of the governing equations are discretized using the following approximation: $(\partial\phi/\partial t)\cong(\phi-\phi^0)/\Delta t$, where ϕ represents a generic dependent variable ($\phi=T$, p, v, x_g, ρ, ...). In the same way, in order to evaluate the axial heat fluxes in the tube wall (cf. *Figure 4*), the spatial derivatives of the temperature are numerically approximated to $(\partial T/\partial z)_e\cong(T_P-T_E)/\Delta z$ and $(\partial T/\partial z)_w\cong(T_W-T_P)/\Delta z$.

The mean values over a control volume of the different variables have been estimated by the arithmetic average between the inlet and outlet sections, that is: $\bar{\phi}\cong\bar{\phi}=(\phi_i+\phi_{i+1})/2$. The mean

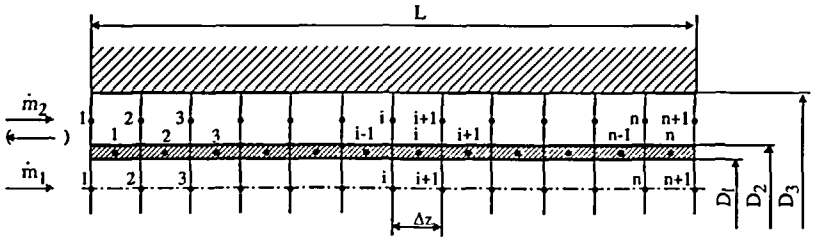

Figure 5 Node distribution along the double-pipe heat exchanger

thermophysical properties have been evaluated at the correspondent mean variables. The enthalpy variations have been evaluated neglecting their dependence on pressure variations, that is: $\Delta h \cong c_p(\bar{T})\cdot\Delta T$.

Single-phase flow. The following equations are applicable, inside the tube of the condenser and the evaporator where the fluid remains in both single-liquid phase and single-vapour phase (regions I and III from *Figure 1*), and also inside the annulus using the hydraulic diameter (D_3-D_2, see *Figure 5*) to evaluate the friction factor and the convective heat transfer coefficient. Applying the numerical approach indicated above, the outlet temperature is obtained from the discretized *energy equation*,

$$T_{i+1}=\frac{a\Delta z(2T_{wall}-T_c)+b_1T_i-b_2+\dfrac{S\Delta z}{\Delta t}[c_1(T_i^0+T_{i+1}^0-T_i)-c_2]}{b_1+\dfrac{S\Delta z}{\Delta t}c_1+a\Delta z} \tag{5}$$

where

$$a=2\bar{\alpha}P \qquad b_1=2\bar{m}c_p \qquad b_2=2\bar{m}\left(\frac{v_{i+1}^2-v_i^2}{2}+g\sin\theta\,\Delta z\right)$$

$$c_1=\bar{\rho}^0c_p \qquad c_2=2\left(\bar{\rho}\frac{v_i^2+v_{i+1}^2-v_i^{02}-v_{i+1}^{02}}{4}-\frac{p_i+p_{i+1}-p_i^0-p_{i+1}^0}{2}\right)$$

the discretized *momentum equation* is solved for the outlet pressure,

$$p_{i+1}=p_i-\frac{\Delta z}{S}\left(\frac{\bar{f}}{4}\frac{\bar{m}^2}{2\bar{\rho}S^2}P+\bar{\rho}Sg\sin\theta+\frac{(\dot{m}_{i+1}v_{i+1}-\dot{m}_iv_i)}{\Delta z}+\frac{\bar{m}-\bar{m}^0}{\Delta t}\right) \tag{6}$$

and finally, the discretized *continuity equation* gives the outlet mass flow rate,

$$\dot{m}_{i+1}=\dot{m}_i-\frac{S\Delta z}{\Delta t}(\bar{\rho}-\bar{\rho}^0) \tag{7}$$

Two-phase flow. In this region the discretized *energy equation* is solved for the outlet vapour quality,

$$x_{g,i+1}=\frac{bx_{g,i}-c_1+c_2\Delta z-d\dfrac{S\Delta z}{\Delta t}}{a} \tag{8}$$

where

$$a=\dot{m}_{i+1}\left(\Delta h_{fg,i+1}+\frac{v_{g,i+1}^2-v_{l,i+1}^2}{2}\right) \qquad b=\dot{m}_i\left(\Delta h_{fg,i}+\frac{v_{g,i}^2-v_{l,i}^2}{2}\right)$$

$$c_1=\bar{m}\left(c_{p,l}(T_{i+1}-T_i)+\frac{v_{l,i+1}^2-v_{l,i}^2}{2}+g\sin\theta\,\Delta z\right) \qquad c_2=\bar{q}P$$

$$d=(\bar{\rho}_g\bar{\varepsilon}_g-\bar{\rho}_g^0\bar{\varepsilon}_g^0)\left(\Delta\bar{h}_{fg}+\frac{\bar{v}_g^2-\bar{v}_l^2}{2}\right)+\bar{\rho}_g^0\bar{\varepsilon}_g^0\left(c_{p,g}(\bar{T}-\bar{T}^0)+\frac{\bar{v}_g-\bar{v}_g^0}{2}\right)$$

$$+\bar{\rho}_l^0(1-\bar{\varepsilon}_g^0)\left(c_{p,l}(\bar{T}-\bar{T}^0)+\frac{\bar{v}_l-\bar{v}_l^0}{2}\right)-(\bar{p}-\bar{p}^0)$$

while the outlet temperature is calculated from the saturation condition,

$$T_{i+1}=T_{sat}(p_{i+1}) \tag{9}$$

the discretized *momentum equation* gives outlet pressure,

$$p_{i+1}=p_i-\frac{\Delta z}{S}\left(\frac{\bar{f}_{tp}}{4}\frac{\bar{\dot{m}}^2}{2\bar{\rho}_{tp}S^2}P+\bar{\rho}_{tp}Sg\sin\theta\right.$$
$$\left.+\frac{\dot{m}_{i+1}[x_{g,i+1}v_{g,i+1}+(1-x_{g,i+1})v_{l,i+1}]-\dot{m}_i[x_{g,i}v_{g,i}+(1-x_{g,i})v_{l,i}]}{\Delta z}+\frac{\bar{\dot{m}}-\bar{\dot{m}}^0}{\Delta t}\right) \tag{10}$$

and the mass flow rate is obtained from the discretized *continuity equation*,

$$\dot{m}_{i+1}=\dot{m}_i-\frac{S\Delta z}{\Delta t}(\bar{\rho}_{tp}-\bar{\rho}^0_{tp}) \tag{11}$$

where $\rho_{tp}=\varepsilon_g\rho_g+(1-\varepsilon_g)\rho_l$.

In terms of the mass flow rate, gas and liquid velocities are calculated:

$$v_{g,i+1}=\frac{x_{g,i+1}\dot{m}_{i+1}}{\rho_{g,i+1}\varepsilon_{g,i+1}S} \qquad v_{l,i+1}=\frac{(1-x_{g,i+1})\dot{m}_{i+1}}{\rho_{l,i+1}(1-\varepsilon_{g,i+1})S} \tag{11}$$

Tube wall. Applying the numerical approximations mentioned above, an equation as follows can be obtained for each node of the grid:

$$aT_i=bT_{i+1}+cT_{i-1}+d \tag{12}$$

where the coefficients are:

$$a=\frac{\lambda_w S}{\Delta z}+\frac{\lambda_e S}{\Delta z}+(\alpha_s P_s+\alpha_n P_n)\Delta z+\frac{S\Delta z}{\Delta t}\rho c_p \qquad b=\frac{\lambda_e S}{\Delta z}$$

$$c=\frac{\lambda_w S}{\Delta z} \qquad d=(\alpha_s P_s \bar{T}_{fluid,tube}+\alpha_n P_n \bar{T}_{fluid,annulus})\Delta z+\frac{S\Delta z}{\Delta t}\rho c_p T_i^0$$

These coefficients are applicable for $2\leqslant i\leqslant n-1$; for $i=1$ and $i=n$ adequate coefficients are used to take into account the axial heat conduction or temperature boundary conditions.

Differentiation between regions

The differentiation between the three main regions existing in both the condensation and the evaporation processes is given by the temperature and the vapour quality. These conditions are:

- Liquid region: $T<T_{sat}$, $p>p_{sat}$, $x_g=0$
- Two-phase region: $T=T_{sat}$, $p=p_{sat}$, $0<x_g<1$
- Vapour region: $T>T_{sat}$, $p<p_{sat}$, $x_g=1$

The saturation temperature T_{sat} varies along the duct due to the pressure drop produced by the friction, the momentum variation and the mass forces (when the heat exchanger is not in a horizontal position).

Using the conditions of differentiation between regions mentioned above, the control volume where transition occurs is detected. In order to evaluate the position of the transition point, two criteria have been tested:

- *Transition criterion 1:* the transition point is assigned to the outlet section of the control volume (assignation to the inlet section or to the middle section would be equivalent criteria).

- *Transition criterion 2:* the control volume is divided into two. The length of the first control volume is calculated from the energy equation, imposing saturated conditions with $x_g=0$ or $x_g=1$ at the outlet section. The length of the second one is calculated by simple difference.

Although the two criteria are numerically equivalent, the numerical results presented in this paper show better performance with the second criterion. Therefore, more accurate results are obtained for a given grid, or alternatively fewer control volumes are required for a given accuracy.

Numerical algorithm

At each time step the solution process is carried out on the basis of a global algorithm that solves in a segregated manner the flow inside the tube, the flow inside the annulus, and the heat conduction in the tube wall. The tube and the annulus are solved on the basis of a numerical implicit scheme, moving forward step by step in the flow direction. In each control volume, the set of governing equations is iteratively solved to calculate, from the known values at the inlet section of the control volume and in the whole control volume at the preceding instant, the conditions at the outlet section. For the tube wall, the set of heat conduction discretized equations is solved using the algorithm TDMA[2]. The convergence of the different iterative loops is controlled using adequate rates of convergency. For example, the convergency of the fluid flow equations is considered to have reached when $|T-T^*|<\delta$ for single-phase flow, and $|x_g-x_g^*|/max(x_g,1-x_g)<\delta$ for two-phase flow, where the superscript $*$ indicates the value of the variable at the previous iteration, and δ is the required precision.

The coupling between the three main subroutines has been performed iteratively following the next three steps:

- *Inside the tube,* the equations are solved considering the tube wall temperature distribution as boundary condition, evaluating the convective heat transfer in each control volume.
- *Inside the annulus,* the same process is carried out.
- *In the tube wall,* the temperature distribution is calculated using the convective heat transfer coefficients evaluated in the preceding steps.

The governing equations corresponding to a steady state situation are the same equations shown above without considering the temporal derivative terms. In order to use the transient algorithm to solve steady situations, a very large time step has been considered; in this manner, all temporal derivative terms become null in the discretized governing equations.

In transient situations, the initial conditions have usually been obtained from the solution in steady state with boundary conditions corresponding to $t=0$. In this way, the initial conditions have a high degree of physical sense and convergency problems are avoided.

Evaluation of the empirical coefficients

A complete list of the empirical coefficients used in the modelization is provided: friction factor, convective heat transfer and void fraction, differentiating the cases of condensing and evaporating flow inside the tube, and annulus flow.

Condensing flow inside the tube. In the *single-phase regions* the convective heat transfer coefficient is calculated using the Nusselt and the Gnielinski[4] equations, for laminar and turbulent regimes respectively. The friction factor is evaluated from the expressions proposed by Churchill (cited by Lin *et al.*[5]).

In the *two-phase region* the convective heat transfer coefficient is calculated using, in the case of stratified flow, the Nusselt equation (cited by Butterworth[6]) with the correction of Jaster and Kosky[7], and in the case of annular flow, the expression proposed by Boyko and Kruzhlin[8]; the equation of Wallis[9] is taken as a differentiation criterion between annular and stratified condensation. The void fraction is estimated from the semi-empirical equation by Zivi[10]. The friction factor is calculated from the same equations as in the case of single-phase flow using a

correction factor according to Lockhart and Martinelli[11], correlated by Chisholm (cited by Hewitt[3]). Using the above mentioned expressions, the convective heat transfer tends to zero as does the vapour quality; the convective heat transfer coefficient is limited by the value corresponding to the single-phase liquid flow.

Evaporating flow inside the tube. In the *vapour region* and the *liquid region* without subcooled boiling (pure liquid convection), both the convective heat transfer coefficient and the friction factor are evaluated from the single-phase expressions mentioned above.

In the case of *subcooled boiling*, the convective heat transfer coefficient and the friction factor are treated separately. For the convective heat transfer, the beginning of the subcooled boiling is estimated according to Frost and Dzakowic[12]; the method proposed by Bergles and Rohsenow[13] is used to consider the transition between pure liquid convection heat transfer and boiling heat transfer, which is evaluated from the correlation proposed by Forster and Zuber[14]. For the friction factor, the point of net vapour generation is estimated according to Saha and Zuber[15]; the friction factor is estimated from the single-phase expressions cited above, with a two-phase Reynolds number evaluated from the homogeneous flow model described by Hewitt[3] and the two-phase viscosity proposed by McAdams (cited by Hewitt[3]), and considering the real vapour fraction proposed by Levy[16].

In the *two-phase region*, before the point of dryout, the convective heat transfer coefficient is evaluated using the expression proposed by Kandlikar[17]. The friction factor and the void fraction are calculated in the same way as in the condensation two-phase flow.

The *post-dryout regime* is considered to begin at $x_g=0.9$ for refrigeration purposes[18]. The convective heat transfer has been evaluated from the correlation developed by Groeneveld[19]. The friction factor and the void fraction are calculated from the single-phase expressions mentioned above using the homogeneous flow model described by Hewitt[3] and the two-phase viscosity proposed by McAdams (cited by Hewitt[3]).

Annulus flow. Both the convective heat transfer coefficient and the friction factor are calculated using the expressions corresponding to single-phase flow inside tubes with the hydraulic diameter.

RESULTS

Results obtained with the modelization developed are presented. Firstly, an analysis of the different numerical aspects is presented, accounting for the two proposed transition criteria, and the discretization parameters ($n, \Delta t, \delta$). Secondly, some illustrative results corresponding to the solution of a condenser and an evaporator working with two different fluids (R-12 and R-134a) are presented. More examples of application have been presented by the authors[20,21], which deal with the thermal and fluid-dynamic behaviour of the evaporating flow through capillary tubes and vapour compression refrigerating units.

Numerical aspects analysis

In order to analyze the influence of the two transition criteria considered and the numerical parameters used in the modelization, results of a condensing flow inside a tube at constant wall temperature are shown. Two cases are presented:

Case 1. Condensation inside a tube at constant wall temperature in steady state. The objective is to compare the performance of the criteria 1 and 2 (cf. *numerical solution*) for the transition between single-phase and two-phase flow. The results presented in *Table 1* are the points where the condensation begins and ends, z_{bc} and z_{ec} respectively, together with the outlet temperature T_0. The relative difference with respect to a grid independent numerical solution is also shown, this reference solution is obtained using the transition criterion 2 with the numerical parameters

Table 1 Numerical results offered by the modelization using the transition criteria 1 and 2. The relative differences with respect to the reference solution are given in brackets

	Transition criterion 1			Transition criterion 2		
n	z_{bc} (m)	z_{ec} (m)	T_0 (C)	z_{bc} (m)	z_{ec} (m)	T_0 (C)
10	0.300	3.000	31.56	0.278	2.754	27.96
	(6.0%)	(8.8%)	(12.4%)	(1.8%)	(0.1%)	(0.4%)
20	0.300	2.850	29.33	0.281	2.756	28.01
	(6.0%)	(3.3%)	(4.1%)	(0.7%)	(0.1%)	(0.2%)
50	0.300	2.820	28.87	0.282	2.758	28.06
	(6.0%)	(2.2%)	(2.8%)	(0.4%)	(0.0%)	(0.0%)
100	0.300	2.790	28.46	0.282	2.759	28.07
	(6.0%)	(1.2%)	(1.4%)	(0.4%)	(0.0%)	(0.0%)
200	0.285	2.775	28.28	0.283	2.759	28.08
	(0.7%)	(0.6%)	(0.7%)	(0.0%)	(0.0%)	(0.0%)
500	0.288	2.766	28.17	0.283	2.759	28.08
	(1.8%)	(0.3%)	(0.3%)	–	–	–
100	0.285	2.763	28.13	–	–	–
	(0.7%)	(0.2%)	(0.2%)	–	–	–
200	0.284	2.760	28.10	–	–	–
	(0.4%)	(0.1%)	(0.1%)	–	–	–

Table 2 Outlet temperature T_0(C) obtained for different number of control volumes n, and different time instants

	t (s)						t (s)				
n	0	50	100	150	200	n	0	50	100	150	200
10	27.97	28.24	28.59	28.88	29.06	10	27.97	28.24	28.59	28.88	29.06
20	28.01	28.50	28.90	29.19	29.38	20	28.02	28.50	28.90	29.19	29.38
50	28.07	28.56	28.95	29.27	29.49	50	28.07	28.56	28.95	29.26	29.49
100	28.07	28.56	28.96	29.27	29.51	100	28.07	28.56	28.96	29.27	29.51
200	28.08	28.56	28.96	29.27	29.51	200	28.07	28.56	28.96	29.27	29.51
500	28.08	28.57	28.96	29.28	29.51	500	28.08	28.56	28.96	29.27	29.51
1000	28.10	28.58	28.99	29.29	29.53	1000	28.08	28.56	28.96	29.27	29.51
2000	28.11	28.60	29.00	29.31	29.55	2000	28.08	28.56	28.96	29.27	29.51
	$\delta = 10^{-5}$, $\Delta t = 12.5$ s						$\delta = 10^{-7}$, $\Delta t = 12.5$ s				

$n = 500$ and $\delta = 10^{-6}$. The case analyzed corresponds to:

- Geometry: $L = 3$ m, $D_1 = 5$ mm, $\theta = 0$, $\zeta/D = 10^{-6}$
- Fluid: R-12
- Boundary conditions: Tube wall: $T_{wall} = 20$ C
  Fluid ($z = 0$): $T_i = 40$ C, $p_i = 8$ bar
  $v_i = 10$ m/s, superheated vapour.

Table 1 shows that the two criteria tested offer an asymptotic solution when the number of control volumes is sufficiently increased. The transition criterion 2 shows much better performance than transition criterion 1. To reach the same precision, 2000 control volumes are required by the transition criterion 1, while only 50 control volumes are required by the transition criterion 2.

From this point on, all results presented are obtained with the transition criterion 2.

Case 2. Condensation inside a tube at constant wall tempearture in transient state. The objective is to analyze the influence of the numerical parameters used in the modelization. *Tables 2* and *3* show the results obtained, in terms of the outlet temperature T_0, for different values of the number of control volumes n, time step Δt, and precision required to finish the

Table 3 Outlet temperature T_0(C) obtained for different time steps Δt, and different time instants

	t (s)						t (s)				
Δt (s)	0	50	100	150	200	Δt (s)	0	50	100	150	200
100	28.08	–	28.96	–	29.51	100	28.07	–	28.95	–	29.51
50	28.08	28.56	28.96	29.27	29.51	50	28.07	28.56	28.96	29.27	29.51
25	28.08	28.56	28.96	29.27	29.51	25	28.07	28.56	28.95	29.27	29.51
12.5	28.08	28.56	28.96	29.27	29.51	12.5	28.07	28.56	28.96	29.27	29.51
6.25	28.08	28.56	28.96	29.28	29.51	6.25	28.07	28.56	28.96	29.27	29.51
3.125	28.08	28.56	28.96	29.28	29.51	3.125	28.07	28.56	28.96	29.27	29.51
1.5625	28.08	28.56	28.96	29.27	29.51	1.5625	28.07	28.56	28.96	29.27	29.51
0.78125	28.08	28.56	28.96	29.28	29.51	0.78125	28.07	28.56	28.96	29.27	29.51
0.39063	28.08	28.55	28.94	29.26	29.49	0.39063	28.07	28.56	28.96	29.27	29.51
0.19531	28.08	28.55	28.95	29.26	29.50	0.19531	28.07	28.56	28.96	29.27	29.51
0.09766	28.08	28.61	29.01	29.32	29.55	0.09766	28.07	28.55	28.95	29.27	29.51
0.04883	28.08	28.53	28.92	29.26	29.49	0.04883	28.07	28.54	28.94	29.27	29.50
	$\delta=10^{-5}$, $n=200$						$\delta=10^{-7}$, $n=200$				

iterative loops δ. The analyzed situation is:

- Geometry: $L=3$ m, $D_1=5$ mm, $\theta=0$, $\zeta/D=10^{-6}$
- Fluid: R-12
- Boundary conditions: Tube wall: $T_{wall}=20$ C
  Fluid (z=0): $T_i(t)=T_\infty+(T_0-T_\infty)\cdot\exp(-t/t_0)$,
  $p_i(t)=p_\infty+(p_0-p_\infty)\cdot\exp(-t/t_0)$,
  $v_i=10$ m/s, superheated vapour
  where:
  $T_0=40$ C, $T_\infty=46$ C, $p_0=8$ bar, $p_\infty=10$ bar, $t_0=200$ s

Tables 2 and *3* show good accuracy even when coarse grids and a relatively high time step are employed. In general, using $n=100\div200$, $\Delta t=50$ s, $\delta=10^{-5}$, grid independent solutions are achieved,

Illustrative results

In this section, the solution of a double-pipe condenser and evaporator working with R-12 and R-134a are presented. The cases analyzed are:

Case 3. Solution of a double pipe condenser, in transient state. The condensing fluids considered are R-12 and R-134a, and the secondary fluid is water. The analyzed situation corresponds to:

- Geometry: $L=3$ m, D_1, D_2, $D_3=6$, 8, 16 mm, $\zeta/D=10^{-6}$, $\theta=0$
- Flow arrangement: counter flow
- Tube: Fluid: R-12 and R-134a
  Boundary conditions ($z=0$):
  $p_i(t)=p_\infty+(p_0-p_\infty)\cdot\exp(-t/t_0)$, where: $p_0=8$ bar, p_∞ 10 bar, $t_0=200$ s,
  $T_i=45$ C, $\dot{m}_i=2.5\cdot10^{-3}$ kg/s, superheated vapour,

Annulus: Fluid: water
Boundary conditions ($z=L$):
$T_i(t)=T_\infty+(T_0-T_\infty)\cdot\exp(-t/t_0)$, where: $T_0=20$ C, $T_\infty=15$ C, $t_0=200$ s,
$p_i=1.5$ bar, $\dot{m}_i=5\cdot10^{-2}$ kg/s.

- Tube wall: Material: copper
  Boundary conditions: adiabatic ends.
- Numerical parameters: $\delta=10^{-6}$, $n=300$, $\Delta t=100$ s.

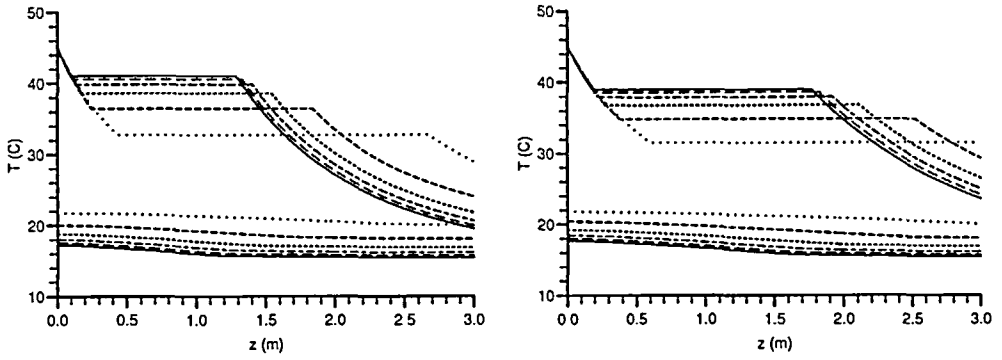

Figure 6 Tube and annulus temperature distribution in a double-pipe condenser at different instants: ···· $t=0$ s, --- $t=100$ s, ---- $t=200$ s, -·- $t=300$ s, -- $t=400$ s, —— $t=\infty$

Figure 6 shows the temperature distribution of the flow inside both the tube and the annulus.

From the figure, a typical logarithmic temperature distribution for the single-phase flow can be observed. The two-phase flow is characterized by a slight temperature drop due to the pressure drop. The behaviour of the two fluids tested (R-12 and R-134a) present small differences. A sudden change in the slope of the annulus temperature can be observed; the reason is that inside the tube, the convective heat transfer coefficient is several times greater in the high vapour quality two-phase region than in the low vapour quality two-phase region and the liquid region.

Case 4. Solution of a double pipe evaporator, in transient state. The evaporating fluids considered are R-12 and R-134a, and the secondary fluid is water. The analyzed situation corresponds to:

- Geometry: $L=3$ m, D_1, D_2, $D_3=6$, 8, 16 mm, $\zeta/D=10^{-6}$, $\theta=0$
- Flow arrangement: counter flow
- Tube: Fluid: R-12 and R-134a
  Boundary conditions ($z=0$):
  $p_i(t)=p_\infty+(p_0-p_\infty)\cdot\exp(-t/t_0)$, where: $p_0=2$ bar, $p_\infty=1.5$ bar, $t_0=200$ s, $T_i=-25$ C, $\dot{m}_i=2.5\cdot10^{-3}$ kg/s, subcooled liquid
- Annulus: Fluids: water
  Boundary conditions ($z=L$):
  $T_i(t)=T_\infty+(T_0-T_\infty)\cdot\exp(-t/t_0)$, where: $T_0=10$C, $T_\infty=15$ C, $t_0=200$ s, $p_i=1.5$ bar, $\dot{m}_i=5\cdot10^{-2}$ kg/s
- Tube wall: Material: copper
  Boundary conditions: adiabatic ends
- Numerical parameters: $\delta=10^{-6}$, $n=300$, $\Delta t=100$ s.

Figure 7 shows the temperature distribution of the flow inside both the tube and the annulus.

As in the case of the condenser, a typical logarithmic temperature distribution for the single-phase flow can be observed; the two-phase flow is characterized by a slight temperature drop due to the pressure drop; and the behaviour of the two fluids tested (R-12 and R-134a) presents small differences. The point of dryout can be detected as the point where the slope of the annulus temperature changes suddenly due to the fall of the convective heat transfer inside the tube in the post-dryout regime.

Computational cost: the condenser and the evaporator solved above have required a computational time consumption of 2 and 20 seconds per time step, respectively, in a workstation

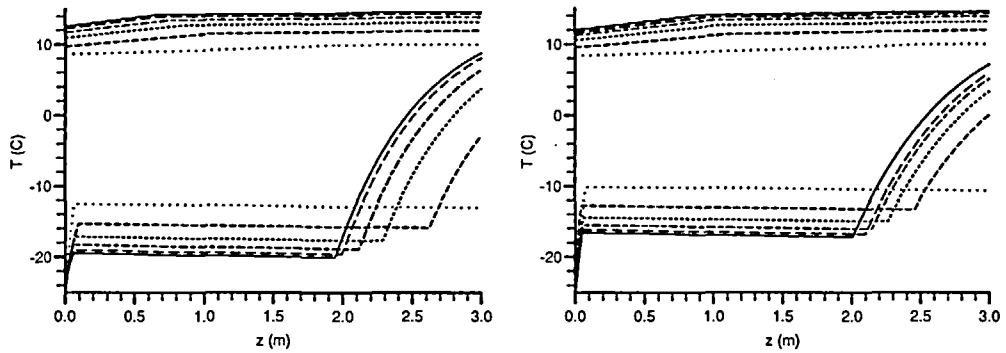

Figure 7 Tube and annulus temperature distribution in a double-pipe evaporator at different instants: ···· $t=0$ s, --- $t=100$ s, ---- $t=200$ s, -·- $t=300$ s, –– $t=400$ s, —— $t=\infty$

of 75 Mips. The refrigerating equipment is characterized by saturated two-phase flow entering the evaporator; in this case, a computational time consumption of only 4 seconds per time step using the same numerical parameters would be required.

CONCLUDING REMARKS

A numerical method for analyzing the behaviour of double-pipe condensers and evaporators has been developed by means of a transient one-dimensional analysis of the fluid flow governing equations (continuity, momentum and energy) and the heat conduction in the tube wall. Empirical information is needed in order to evaluate shear stress, heat flux and two-phase flow structure.

The simulation has been implemented on the basis of an implicit step by step numerical scheme for the fluid flow inside the tube and the annulus, and an implicit central difference numerical scheme in the tube wall, solved by means of the Tri-Diagonal Matrix algorithm (TDMA). The three zones are solved iteratively in a segregated manner.

In order to minimize computational time consumption, a special treatment has been implemented solving the control volume that contains the transition from single to two-phase flow and vice versa. A study of the influence of the numerical parameters used in the modelization shows that accurate numerical results are achieved even when using a small number control volumes and a relatively high time step, and a reasonable computational cost is obtained. The modelization can be a helpful tool to design thermal units that include double-pipe condensers and evaporators.

ACKNOWLEDGEMENTS

This study has been supported by the company Unidad Hermética S.A. (group Electrolux Compressors), by the Comisión Interministerial de Ciencia y Tecnología, Spain (Ref. no. PTR-90060), by the Dirección General de Investigación Científica y Técnica, Spain (ref. no. PB90-0606), and by the Direcció General d'Universitats, Catalonia, Spain (Program AD1).

The authors thank J. M. Serra, J. Pons, A. Castillo, of Unidad Hermética S.A. for the technical support given.

REFERENCES

1 Collier, J. G. *Convective Boiling and Condensation*, 2nd edn, McGraw-Hill, New York (1981)
2 Patankar, S. V. *Numerical Heat Transfer and Fluid Flow*, Hemisphere Publishing Corporation, Washington, D.C. (1980)
3 Hewitt, G. F. Gas-liquid flow, *Heat Exchanger Design Handbook*, **sec. 2.7.3**, ed. by E. U. Schlünder *et al.*, Hemisphere Publishing Corporation, Washington (1983)
4 Gnielinski, V. 'Forced convection', *Heat Exchanger Design Handbook*, **sec. 2.5.1**, ed. by E. U. Schlünder *et al.*, Hemisphere Publishing Corporation, Washington (1983)
5 Lin, S., Kwok, C. C. K., Li, R. Y., Chen, Z. H. and Chen, Z. Y. 'Local frictional pressure drop during vaporization of R-12 through capillary tubes, *Int. J. Multiphase Flow*, **17** (1), 95–102 (1968)
6 Butterworth, D. Film condensation of pure vapor, *Heat Exchanger Design Handbook*, **sec. 2.6.2**, ed. by E. U. Schlünder *et al.*, Hemisphere Publishing Corporation, Washington (1983)
7 Jaster, H. and Kosky, P. G. Condensation heat transfer in a mixed flow regime, *Int. J. Heat and Mass Transfer*, **19**, 95–99 (1976)
8 Boyko, L. D. and Kruzhilin, G. N. Heat transfer and hydraulic resistance during condensation of steam in a horizontal tube and in a bundle of tubes, *Int. J. of Heat and Mass Transfer*, **10**, 361–373 (1969)
9 Wallis, G. B. *One-Dimensional Two-Phase Flow*, McGraw-Hill Book Company, New York (1969)
10 Zivi, S. M. Estimation of Steady-State Steam Void Fraction by Means of the Principle of Minimum Entropy Production, *J. of Heat Transfer*, **86C**, 247–252 (1964)
11 Lockhart, R. W., Martinelli, R. C. Proposed Correlation of Data for Isothermal Two-Phase, Two-Component Flow in Pipes, *Ch. Eng. Progress*, **45 no 1**, 39–48 (1949)
12 Frost, W., Dzanowic, G. S. An Extension of the Method of Predicting Incipient Boiling on Commercially Finished Surfaces, *ASME/AIChE Heat Transfer Conf*, **paper 67-ht-61**, 1–8, Seattle (1967)
13 Bergles, A. E., Rohsenow, W. M. The determination of forced-convection surface-boiling heat transfer, *J. Heat Transfer*, **86C**, 365–372 (1964)
14 Forster, H. K. and Zuber, N. Dynamics of vapour bubble growth and boiling heat transfer, *AIChE J*, **1 no 4**, 531–535 (1955)
15 Saha, P. and Zuber, N. Point of net vapour generation and vapour volumetric void fraction, *Proc. 15th Int. Heat Transfer Conf*, **paper B4.7**, 175–179 (1974)
16 Levy, S. Forced convection subcooled boiling prediction of vapour volumetric fraction, *Int. J. Heat Mass Transfer*, **10**, 951–965 (1967)
17 Kandlikar, S. G. A model for correlating flow boiling heat transfer in augmented tubes and compact evaporators, *J. of Heat Transfer*, **113**, 966–972 (1991)
18 *ASHRAE Handbook, 1981 Fundamentals*, ASRAE Inc, Atlanta (1982)
19 Groeneveld, D. C., Post-Dryout Heat Transfer at Reactor Operating Conditions, *Natl. Topical Meet. Water Reactor Safety*, **ANS paper AECL-4513**, 321–350, Utah (1973)
20 Escanes, F., Pérez-Segarra, C. D., Oliva, A. 'Numerical simulation of capillary tube expansion devices', to be published at the *Int. J. of Refrigeration*
21 Escanes, F., Oliva, A., Pérez-Segarra, C. D. and Flores, F. J. Numerical simulation of a single stage vapor compression refrigerating unit', *Int. Compressor Engineering Conf. at Purdue*, **1**, 139–144, ed. by W. Soedel, Purdue University, IN (1994)